PNAS RESEARCH ARTICLE | ECOLOGY

Tree growth after a major hurricane reflects predisturbance vigor rather than canopy damage

Laura E. Boeschoten[a,b,1], Roi Ankori-Karlinsky[a], Gabriel Arellano[c,d], Alyssa J. Brown[a], Dingyi Fang[e], Veronika Leitold[f], Douglas Morton[g], Gan Yuan[h], Tian Zheng[e], Jess K. Zimmerman[i], and María Uriarte[a]

Affiliations are included on p. 10.

Edited by Rodolfo Dirzo, Stanford University, Stanford, CA; received November 10, 2025; accepted March 13, 2026

Tree crown damage from disturbance events strongly influences forest demography, yet its effect on stem growth remains poorly quantified, with both positive and negative impacts reported. Hurricanes provide a powerful natural experiment to examine these dynamics, generating a broad range of structural damage across individuals and forest stands. Here we assess how crown damage from Hurricane María (2017) affected poststorm stem growth in a wet subtropical forest in Puerto Rico by combining airborne LiDAR with field measurements for 1,082 trees. Unlike previous studies, paired pre- and posthurricane LiDAR assessment enabled us to quantify crown damage as a continuous, objective variable across the canopy. Using a causal inference framework, we separated individual- from neighborhood-level effects, defined as the damage that occurred within a 5 m radius of each tree. Repeated stem growth censuses allowed direct comparison of individual growth responses before and after the hurricane. Across the community, posthurricane stem growth rates were similar to prehurricane values. Larger and more heavily damaged trees exhibited moderately reduced growth, while neighborhood crown damage and mortality had no detectable effect. However, these damage effects were smaller than the influence of prehurricane growth rates, indicating that prehurricane individual vigor outweighed biomass loss and competitive release in shaping growth responses. These findings highlight the resilience of surviving trees in sustaining carbon uptake after a severe disturbance and challenge the assumption of strong postdamage growth suppression that is embedded in dynamic vegetation models.

cyclone | crown damage | competitive release | forest disturbance | LiDAR

Significance

Severe storms are expected to intensify with climate change, yet the long-term impacts of hurricane damage on tropical tree growth remain a subject of debate. By integrating airborne Light Detection and Ranging (LiDAR) with repeated field measurements for 1,082 trees in Puerto Rico, we provide an assessment of how continuous, individual-level crown damage from a major hurricane affected stem growth. Our causal inference approach allowed us to explicitly separate focal-tree from neighborhood damage and incorporate predisturbance growth. Contrary to expectations, predisturbance growth was a stronger predictor of poststorm growth than biomass loss or competitive release. Our findings highlight the resilience of surviving trees in this hurricane-prone forest and demonstrate that modeling large-scale disturbance effects must account for local context and individual responses.

Crown damage is a common outcome of forest disturbances and can affect tree demography long after the event (1, 2). By reducing biomass and leaf area, damage influences delayed survival and growth, leaving long-lasting legacies in forest structure (3–6). These disturbances play a central role in shaping forest dynamics and affect key ecosystem processes, including carbon storage, water cycling, and nutrient fluxes (7–10). As climate change is projected to intensify storms, pests, and other disturbance agents, crown damage will likely become even more widespread (11–13). Yet despite growing insights into how damage shapes mortality (2, 14, 15), its effects on growth remain poorly understood, even though growth is fundamental to long-term carbon sequestration and ecosystem resilience (16).

The limited empirical evidence on how crown damage shapes tree growth constrains our ability to represent these effects in models (1, 17), even though capturing such disturbance legacies is crucial for predicting how forests will respond to global change (18). Current vegetation demographic models highlight this gap. While some modeling approaches have begun to incorporate both the immediate and delayed effects of damage on mortality (19–22), comparable representations of damage effects on growth remain limited. An example is ELM-FATES, a dynamic global vegetation model that simulates how individual trees grow, compete, die, and respond to disturbance within an Earth system modeling context. In its representation of disturbance, biomass loss directly reduces stem growth, based on observations from a Panamanian forest that is unaffected by large-scale disturbances (1). This relationship may not hold in disturbance-prone ecosystems, where species have evolved under recurrent disturbance regimes and may possess traits that promote resilience (23, 24).

Hurricanes (also referred to as cyclones or typhoons) offer a valuable natural experiment for studying the effects of crown damage on tree growth, addressing this knowledge gap. In tropical regions, these storms cause widespread canopy opening and biomass loss across both coastal and inland forests (7, 25, 26). Because hurricanes generate a wide range of damage severity, both to individuals and their neighbors, they create an ideal setting to

Author contributions: L.E.B. and M.U. designed research; L.E.B., R.A.-K, G.A., A.J.B., D.F., V.L., D.M., G.Y., T.Z., J.K.Z., and M.U. performed research; L.E.B. analyzed data; and L.E.B. and M.U. wrote the paper.

The authors declare no competing interest.

This article is a PNAS Direct Submission.

[1]To whom correspondence may be addressed. Email: laura.boeschoten@ugent.be.

This article contains supporting information online at https://www.pnas.org/lookup/suppl/doi:10.1073/pnas.2532451123/-/DCSupplemental.

Published April 13, 2026.

evaluate how tree growth scales with varying levels of individual and neighborhood damage (4). Field studies of hurricanes show that crown damage can influence stem growth in opposing ways. Growth rates in surviving trees may increase after a storm (3, 5, 27, 28), either because neighborhood mortality reduces competition, which positively impacts the focal tree ("competitive release"), or because branch loss stimulates new growth by a pruning effect. Conversely, extensive loss of biomass from the canopy can reduce photosynthetic capacity and suppress growth ("biomass loss"), sometimes compounded by increased heat stress or additional storm effects such as salt intrusion in coastal forests (29–31). These contrasting mechanisms, competitive release versus biomass loss, often occur simultaneously, complicating efforts to disentangle their contributions. Previous studies, while spanning a range of storm intensities, still relied on categorical indices of damage severity (e.g., ref. 32) because data for predisturbance crown conditions were not available (3, 33). Yet crown damage severity is likely a key determinant of whether growth is stimulated or suppressed. With more precise measurements of individual- and neighborhood-level damage, we can better study the relative importance of competitive release versus biomass loss.

Small-footprint airborne LiDAR offers a potential solution to quantify prehurricane forest structure and storm damage. By providing three-dimensional data on forest structure, repeated pre- and postdisturbance LiDAR surveys provide robust, quantitative measures of canopy loss and recovery at the individual tree level, including height loss and crown expansion (34). This approach enables estimation of direct damage to focal trees and to the surrounding neighborhoods, helping to separate damage-driven growth reductions from competitive release. When integrated with repeated field measurements of stem growth, LiDAR-derived canopy metrics allow for a more comprehensive quantification of postdisturbance growth dynamics, revealing patterns of damage and recovery difficult to detect through field methods alone. Together, remote and field-based observations can thus provide unique insights into the complex, multiscale impacts of hurricanes on forest structure and stem growth (35). Additionally, comparing LiDAR-based estimates with categorical assessments of field damage provides an additional test of robustness, as each method carries limitations: field surveys rarely include prehurricane baselines, while LiDAR faces challenges in accurately delineating crowns and matching them to individual stems on the ground. By combining these complementary approaches, each with its own uncertainties, we can gain confidence if the two methods converge on similar results.

In this study, we use a time series of airborne LiDAR data to assess the impact of Hurricane María, a category 4 storm, on stem growth in a subtropical forest in Puerto Rico. Our goal is to identify which aspects of damage most strongly influence posthurricane stem growth in canopy trees. In particular, we aim to distinguish the effects of individual crown damage from neighborhood damage (Fig. 1). We used two complementary measures to assess the impact of hurricane damage on stem growth: absolute growth posthurricane and stem growth change (posthurricane/prehurricane growth ratio). Both measures provide distinct but valuable insights into the effects of hurricane damage. Absolute growth highlights the overall "winners" after the hurricane by identifying which trees grew the most across the community. Stem growth change, on the other hand, captures individual-level responses: how a given tree's growth shifted posthurricane and which factors influence the extent of that shift.

H. María made landfall in September 2017 as the most powerful hurricane to strike the island since 1928 (36), delivering sustained winds up to 250 km/h and 500 mm of rainfall within 24 h. It caused widespread forest damage, including extensive stem breakage in species typically considered resistant due to high wood density (25). The long-term effects of this storm are still unfolding, making H. María a benchmark for assessing how intensifying hurricanes under climate change will alter forest dynamics. Here, we combine data from three LiDAR acquisitions [2017, 2018, 2020 (34)] with field assessments of damage and stem growth before and after the hurricane. This unique continuous, individual-level and neighborhood-level assessment of crown damage allows us to address the following questions and test the associated hypotheses:

1) What is the effect of a hurricane on community-wide stem growth of canopy trees following the event? We anticipate that posthurricane stem growth rates will increase compared to prehurricane conditions in this wet subtropical forest, consistent with observations from other wet forests affected by hurricanes (3, 5). This expected increase aligns with the hypothesis that hurricane damage reduces competition among surviving stems, thereby enhancing their growth.
2) What is the impact of individual crown damage, quantified as crown height lost, on changes in stem growth relative to prehurricane conditions? We hypothesize that crown height loss has a nonlinear effect on posthurricane stem growth change. Small to moderate height loss may have a positive effect because of a reduction in respiration costs, allowing trees to reallocate resources and increase stem growth. However, when damage is too extensive, the loss of photosynthetic capacity is expected to reduce growth.
3) What are the relative effects of focal tree and neighborhood damage on both absolute stem growth and relative change in stem growth posthurricane (post/pre-growth ratio)? We expect that crown height loss will be the strongest predictor due to its direct effect on a tree's ability to photosynthesize and produce sugars necessary for growth. In contrast, neighborhood damage might either promote growth, by reducing competition, or suppress growth through increased exposure to heat and light stress. Since growth also reflects environmental conditions, we also considered topography in the analyses, a known driver of tree demography at the site (37). We expect that trees situated on steep slopes or in areas with a high topographic wetness (leading to anoxic soils) will show slower recovery, resulting in a more negative relative stem growth response.
4) How do these impacts in stem growth change vary among species with different life history strategies? We expect species with fast life-history strategies (pioneers) to benefit most from the increased light availability after a hurricane, showing the strongest gains in relative stem growth change. On the other hand, we expect that resilient long-lived pioneers (23), which dominate this forest and have evolved with frequent disturbances, will show limited effects of hurricane damage.

Results

Our final dataset consisted of 1,082 trees from 19 species that were established in the canopy in 2016 and then survived H. María in September 2017 through the next census (2021–2023), 4 to 6 y later. The mean DBH of these trees was 42 cm (SD ±38.8). Average recorded height loss was moderate: the surviving trees lost a mean of 27% of their height (SD ±17%), with losses ranging from 0 to 86% (*SI Appendix*, Table S1). In absolute terms, this height loss percentage corresponds to a mean height loss of 5.3 m (SD ±3.4), slightly less than the 7.1 m average recorded for the Luquillo Experimental Forest as a whole and the 6.5 m loss that

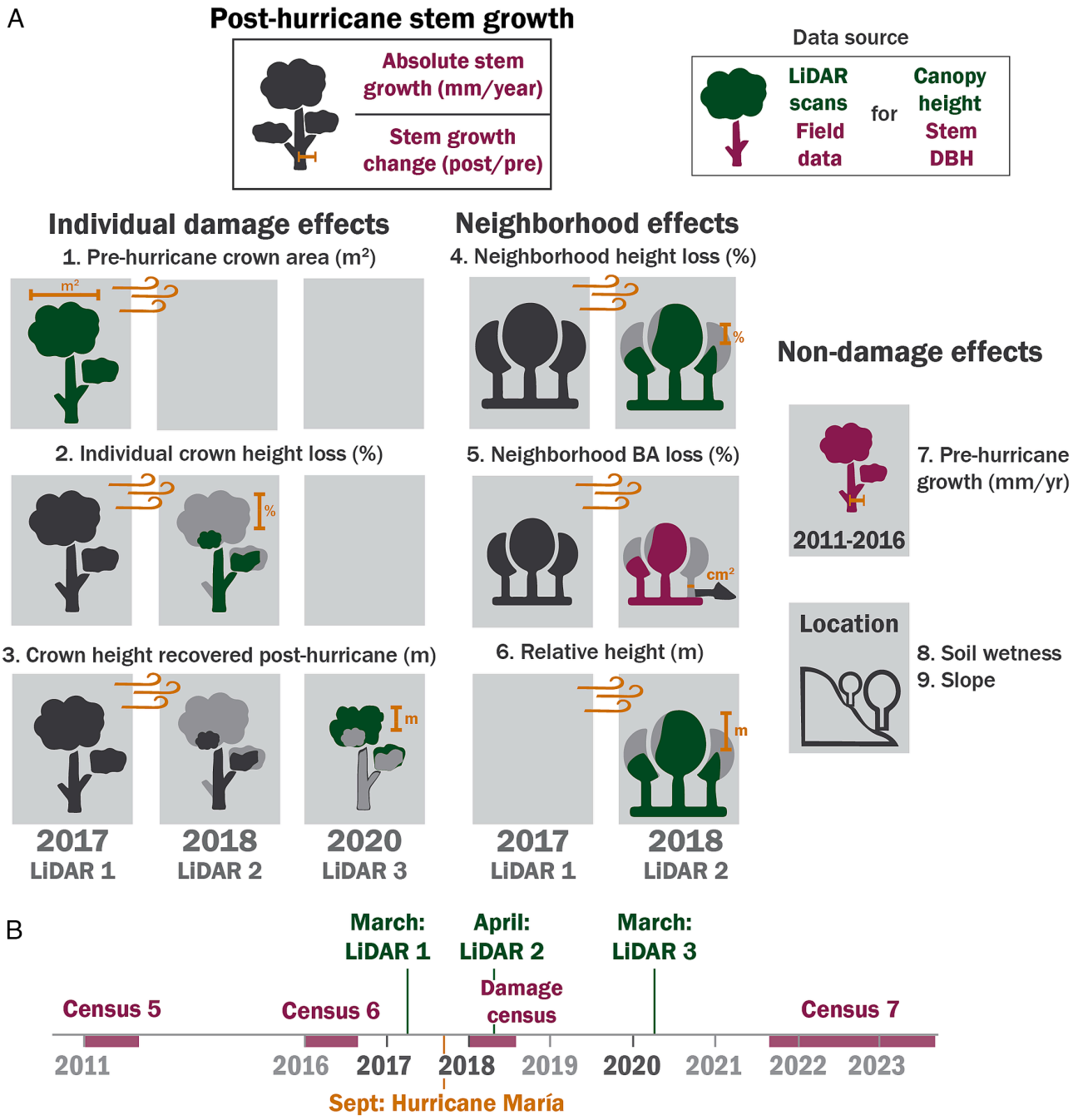

Fig. 1. (*A*) Schematic representation of variables tested for their effect on posthurricane stem growth (absolute and stem growth change). Variables are categorized into individual-level damage effects, neighborhood-level damage effects, and nondamage effects. We evaluated all damage-related variables in relation to both absolute stem growth and stem growth change (the ratio of posthurricane to prehurricane growth). Variables estimated from the LiDAR canopy scans are depicted in green, variables estimated from the field censuses are depicted in purple. Years shown correspond to LiDAR-derived canopy height measurements, with the hurricane occurring between the 2017 and 2018 surveys. From the nondamage variables, the effect of prehurricane growth (7) was tested only for absolute stem growth, as it is already incorporated in the denominator of stem growth change. The causal diagram of the hypothesized interactions is provided in *SI Appendix*, Fig. S1 and corresponding effect sizes are shown in Fig. 4. See *Materials and Methods* for the calculation of the different variables. (*B*) Timeline of events with field censuses measuring diameter at breast height (DBH) of all stems in purple, LiDAR scans from which canopy height was estimated in green and hurricane María in yellow.

was reported for the Luquillo Forest Dynamics Plot (LFDP) in that study (34).

Posthurricane Growth Follows Prehurricane Growth. At the community level, we found no significant effect of Period (pre- or posthurricane) on growth: the credible interval overlapped with zero (95% CI = −0.46 to 0.33) with a mean effect of −0.06. Only *Cordia sulcata* showed a significant positive Period × Species interaction (mean = 0.91, 95% CI = 0.31 to 1.53; Fig. 2). Across individuals, posthurricane responses were heterogeneous: 622 trees exhibited equal or reduced stem growth compared to prehurricane rates, while 493 showed increased growth.

The Dominant Drivers of Posthurricane Growth. Contrary to our expectation, we detected a small linear effect of percentage height loss on stem growth change rather than a nonlinear effect

(Fig. 3), as the credible interval of the quadratic part of the model overlapped with zero (mean estimate = 0.022, CI = −0.002 to 0.045). Therefore, we removed the quadratic term from the final models. However, we found a small linear negative effect of percentage height loss (mean = −0.05, 95% CI = −0.10 to −0.01, Fig. 4*B*).

We next compared the various effects of hurricane damage on stem growth (Fig. 1) based on the Directed Acyclic Graph (DAG) (*SI Appendix*, Fig. S1) and corresponding models (*SI Appendix*, Table S2). Prehurricane growth emerged as the best predictor of posthurricane growth (Fig. 4*A*), after accounting for tree size, by including crown area as a covariate in the primary model. An alternative model using DBH instead of crown area produced similar results, confirming that this effect of prehurricane vigor was not simply due to tree size.

Trees that were taller than their neighbors after the hurricane (higher posthurricane relative height difference, m) exhibited slightly higher absolute stem growth. In contrast, we found no effect of prehurricane crown area (m^2), tree height loss (%), crown height recovered (m), neighborhood height loss (%), or neighborhood basal area loss (%) on absolute stem growth.

For stem growth change, we detected significant negative effects of both prehurricane crown area (m^2) and percentage tree height loss (Fig. 4*B*). In contrast, height recovered (m), neighborhood height loss (%), neighborhood basal area loss (%) and relative height were not associated with stem growth responses. Of the topographic variables, we found a small negative effect of topographic wetness index (TWI) on absolute stem growth and a small positive effect of slope (% angle).

Species Differences in Stem Growth Change. We found differences among species in stem growth change (Fig. 5; Kruskal–Wallis rank sum test, chi-square = 36.1, df = 19, P = 0.01). Post hoc pairwise comparisons showed that differences among species were

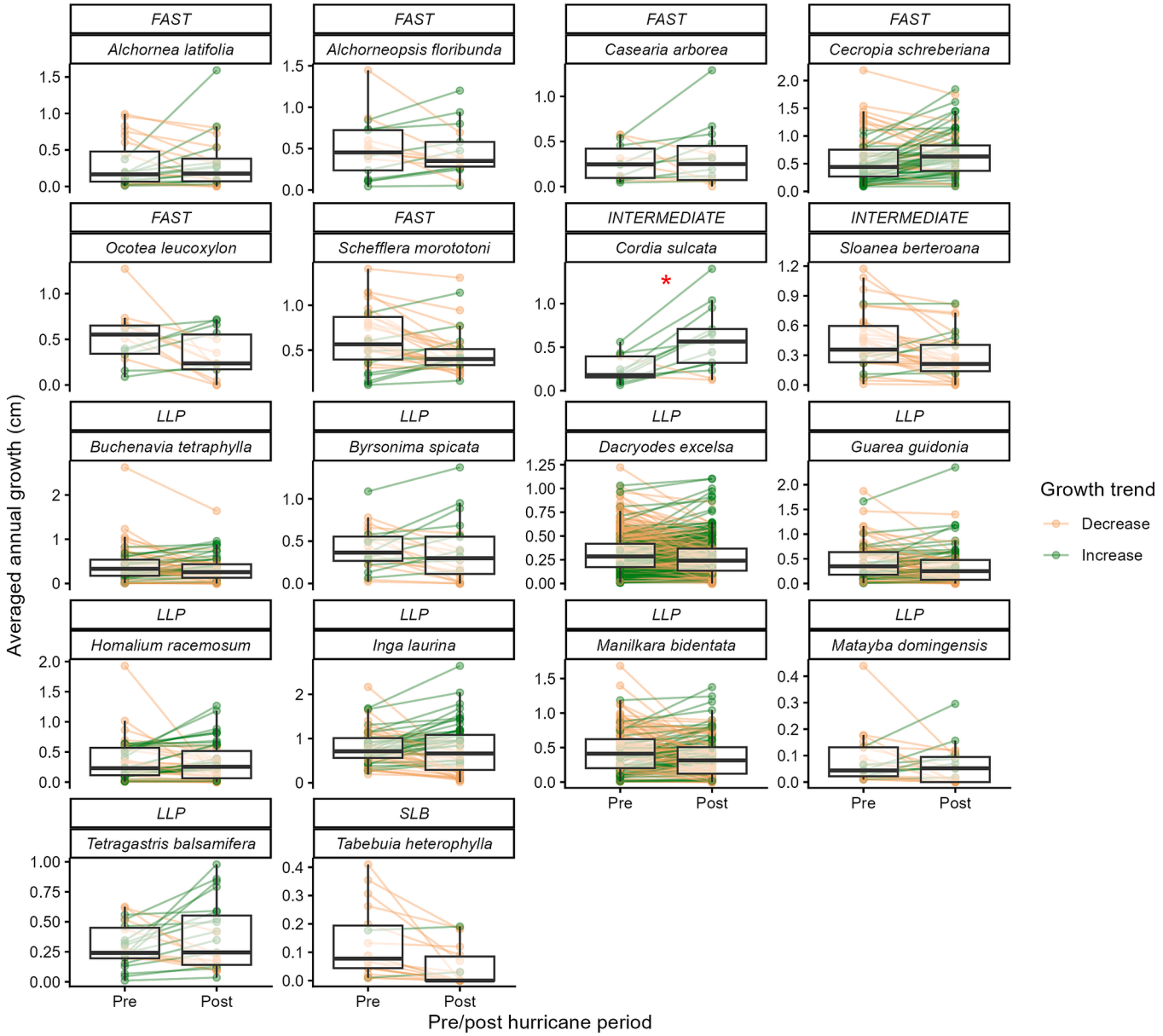

Fig. 2. Annual stem growth estimates from prehurricane (2011–2016) and posthurricane (2016–2021–2023) census intervals shown by species and ordered by demographic strategy (LLP = long lived pioneer; SLB = short lived breeder). Lines connect repeated measurements of pre- and posthurricane growth for individual trees, colored by whether posthurricane growth increased or decreased relative to prehurricane growth. A red asterisk indicates a significant Period × Species interaction indicating a different growth trend after the hurricane (*Methods and Materials*).

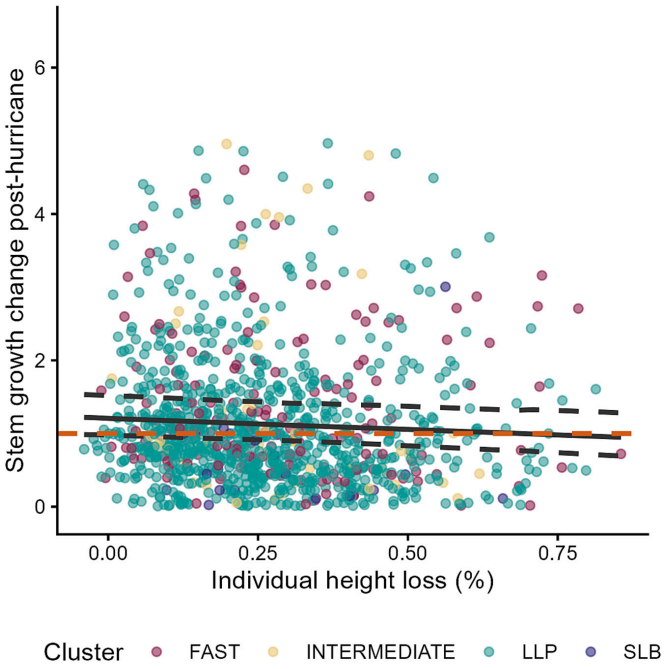

Fig. 3. The effect of individual crown height loss (%) on stem growth change posthurricane (unit-less). Stem growth change is calculated as post/pre-hurricane growth ratio, values >1 (orange dotted line) indicate increased growth in the posthurricane period. Individual height loss is calculated from the canopy height models (CHM) based on the LiDAR scans in 2017 and 2018. Individuals are colored by their species' demographic strategy, LLP = long lived pioneer; SLB = short lived breeder. The significant linear effect of height loss (%) on stem growth change is indicated by the thick continuous line, with the 95% credible interval as dotted lines.

spread across the different life history strategy clusters. *Cecropia schreberiana*, a dominant fast-growing species in this forest, had a significantly higher increase in stem growth than about half of the other species, most of which showed no change or a slight reduction in average stem growth, but the other species with a fast strategy exhibited less distinct growth changes and the fast-growing species *Ocotea leucoxylon* even showed reduced growth posthurricane.

Discussion

With disturbance events increasing in frequency and intensity globally (13), we need a better understanding of how crown damage affects forest resilience. This study provides an assessment of postdisturbance stem growth of surviving trees that uses a continuous measure of crown damage, quantified as percentage crown height loss, rather than traditional categorical damage classes. Furthermore, adopting a causal inference framework allowed us to separate individual- from neighborhood-level effects. We found moderately reduced growth after disturbance for larger and more severely damaged trees. Crucially, the impact of individual-level and neighborhood damage was smaller than the influence of pre-hurricane growth rates, indicating that prehurricane tree vigor is a stronger predictor of postdisturbance growth than biomass loss. These findings have important implications for modeling forest recovery, suggesting that trees that exhibited high growth rates prior to the hurricane continued to do so postdisturbance.

At the community level, we did not find an increase in post-hurricane stem growth (Fig. 2), in contrast to findings from other wet forests affected by less severe hurricanes (3, 5, 27). The exceptionally severe damage caused by H. María (25), which killed 974 of the 3,501 identified stems, may have opened the canopy to such an extent that increased heat and water stress outweighed the benefits of competitive release (34). As storm intensity is expected to rise under climate change (11, 38), such outcomes may become increasingly common. Alternatively, canopy trees may have already been growing near their physiological limits, preventing further growth gains. Despite the lack of a community-wide response, individual trees showed substantial variation, reflecting the heterogeneity in damage severity and underscoring the dynamic nature of growth responses after the hurricane. The only species with a significant growth increase was *C. sulcata*, a small tree that benefits from increased light and therefore likely responded positively to posthurricane canopy opening. Prehurricane growth was the strongest predictor of absolute posthurricane growth across all individuals, implying that trees already exhibiting fast growth prior to the disturbance continued to do so regardless of damage.

This finding is consistent with the concept of ecological memory, in which survivors retain physiological and structural resilience that mediates their postdisturbance performance (39), underscoring that historical performance matters (37, 40). Such resilience may be mediated by stored nonstructural carbohydrates that buffer trees against temporary reductions in photosynthetic capacity (41, 42). Consistent with this mechanism, dominant, long-lived species in this forest, such as *Dacryodes excelsa* and *Manilkara bidentata*, exhibited minimal differences between pre- and posthurricane growth (Fig. 5), suggesting that trees that exhibited high growth rates prior to the hurricane continued to do so postdisturbance. These results highlight a positive outlook for this forest: surviving canopy stems, even when exposed to a category 4 hurricane, appear capable of sustaining growth rates comparable to prehurricane levels, supporting carbon uptake and storage.

We did not find an effect of crown height loss on absolute posthurricane stem growth (Fig. 4*A*), indicating that across all individuals, the most heavily damaged trees did not necessarily grow less in stem diameter. In contrast, crown height loss negatively affected stem growth change relative to prehurricane rates (Fig. 4*B*), indicating that individuals that had lost a greater percentage of their crown height experienced stronger growth reductions. This result supports the hypothesis that limited crown damage may act as a pruning effect leading to higher growth rates (3), whereas extensive damage is linked to high photosynthetic tissue losses, suppressing growth (1, 43). However, this effect was linear rather than the hypothesized quadratic. This negative effect of damage on stem growth change was also confirmed by the field-based categorical damage assessment (*SI Appendix*, Fig. S5).

The absence of a nonlinear relationship further suggests that there was no clear threshold of crown height loss beyond which trees exhibit substantially lower growth rates. Surviving individuals experienced a broad range of crown height loss (0 to 86%), indicating large variation in damage for trees that survived the storm. However, these results must be interpreted in the context of survivorship bias: trees that suffered the most severe damage likely died and are therefore missing from our dataset, suggesting that growth reductions for the hardest-hit individuals may be underestimated. Mortality was higher for species in the fast strategy group compared to others, but the range and maximum crown loss of survivors was similar across all species (*SI Appendix*, Table S1). Since our focus is on surviving trees, this survivor-based perspective remains appropriate for characterizing long-term recovery trajectories.

In this context, it is also important to note that we measured cumulative growth over a 5.5 to 7-y period. Although our statistical models accounted for variation in census intervals among individuals, this long time span captures the net growth response rather than immediate postdisturbance effects. Consequently,

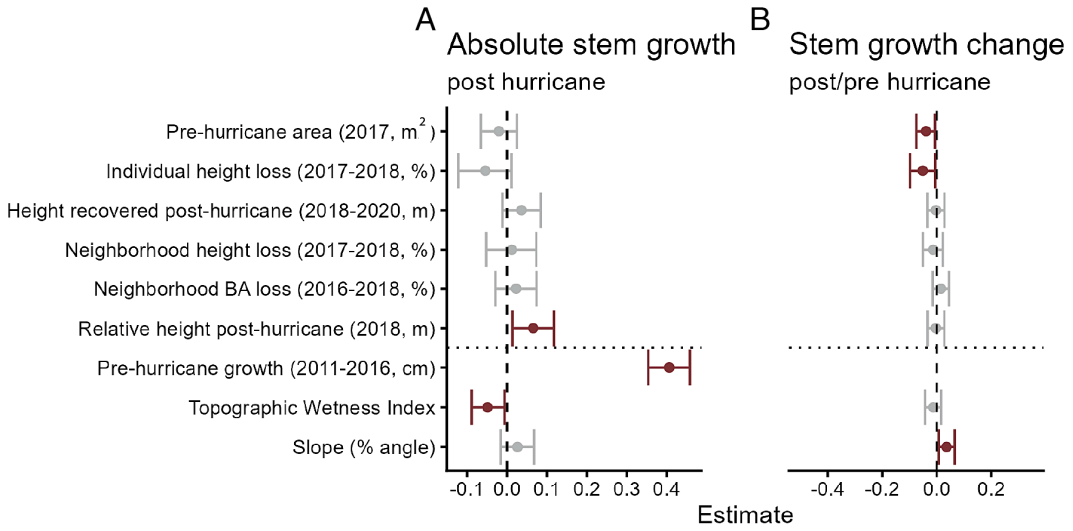

Fig. 4. Estimated standardized effect sizes of damage effects on (*A*) absolute stem growth (cm/y) and (*B*) stem growth change posthurricane (unit-less). Model results are shown as posterior mean coefficients with 95% credible intervals. Please refer to *SI Appendix*, Table S2 for model descriptions and *SI Appendix*, Figs. S6 and S7 for the posterior predictive checks. Variables in red indicate the credible interval does not overlap zero (indicating a strong effect), or in gray when it does (indicating no detectable effect). We did not test for an effect of prehurricane growth on stem growth change, as it is included in the denominator of that response variable. BA loss = Basal Area loss due to mortality

short-term responses, such as growth suppression due to severe defoliation or structural damage, or rapid growth increases driven by higher light availability and reduced neighborhood competition in lightly damaged trees, are not resolved individually but integrated over time. This longer-term perspective is useful for understanding sustained trends (3, 5), but it may also help explain why our results differ from studies that reported positive (3, 27, 28) or negative (30, 31) growth responses in the same year as, or in the years following, a hurricane. Notably, the few studies using tree-ring data, which provide annually resolved growth, documented growth suppression in the hurricane year but did not show a strong growth increase in subsequent years relative to long-term trends (30, 31). This pattern suggests that compensatory growth after severe disturbance may be limited.

Regarding stem growth change, we also found a small but consistent negative effect of prehurricane crown area (m^2, Fig. 4*B*), indicating that larger trees experienced stronger growth reductions following crown damage than smaller individuals. This suggests that canopy loss disproportionately affects larger trees. A potential explanation is that bigger individuals have higher respiration costs associated with maintaining extensive woody tissue and larger root systems (44). These costs remain even when crown damage reduces photosynthetic capacity. Although foliage loss lowers overall respiration, the remaining tissues still require substantial metabolic maintenance, placing larger trees at a relative disadvantage compared to smaller ones.

We found no clear effect of neighborhood crown height loss on either absolute or stem growth change (Fig. 4). This lack of a clear relationship likely reflects the balance between opposing mechanisms. While neighborhood damage can reduce competition and promote growth (4), canopy openings can also elevate local temperatures and exacerbate drought stress, suppressing growth. These counteracting processes likely acted simultaneously, producing only modest net effects. Additionally, individuals that were most affected by neighborhood damage may also have died between censuses, again highlighting survivor bias in this analysis. While this limitation is consistent with the study's aims, it may have reduced the availability of data for highly disturbed neighborhoods.

An alternative explanation for the absence of an effect of neighborhood crown height loss is the rapid infilling of hurricane-created gaps through vertical growth of surviving individuals and recruitment of new understory trees, which is also an important component of posthurricane recovery and ecosystem resilience. Other census-based studies on hurricane damage impacts on growth also included noncanopy individuals (3, 5) and indeed found that smaller individuals showed a smaller to no growth suppression than the big trees (5). Canopy photos and CHM from 2020 support this idea, showing notable crown recovery just 2.5 y after the disturbance (34). This may have been facilitated by the fast recovery of the dominant palm in this forest, *Prestoea acuminata*, which is very resistant to damage (8). In this scenario, only some individuals of the fastest-growing species, such as *C. schreberiana* and *C. sulcata*, may have fully taken advantage of the brief posthurricane window of reduced competition and increased light availability. This finding is in line with earlier work showing that *C. schreberiana* developed larger crowns in areas that were more severely damaged by an earlier hurricane (in 1989) (45).

Across species, some showed higher mean growth after the hurricane while others declined (Fig. 5), but these patterns did not align clearly with life-history strategies or plant functional types commonly represented in demographic vegetation models (Fig. 5). It is likely that species in this forest, which have experienced recurrent disturbances, possess other traits not captured by standard demographic classifications (24). These may include mechanical traits that reduce hurricane damage or enhanced carbohydrate storage capacity that enables rapid recovery after disturbance.

Among the variables related to the growth environment of these trees, we found a small significant positive effect of slope (% angle) on stem growth change and a negative effect of TWI on absolute stem growth (Fig. 4). A possible reason for these effects is that steeper terrain increases light exposure and alleviates the anoxic soil conditions often found in this forest (46). These findings suggest that topography can mediate recovery trajectories of surviving trees to a small degree, with steeper slopes conferring an advantage for posthurricane growth.

Overall, these findings have important implications for modeling forest recovery following major disturbances. Current models

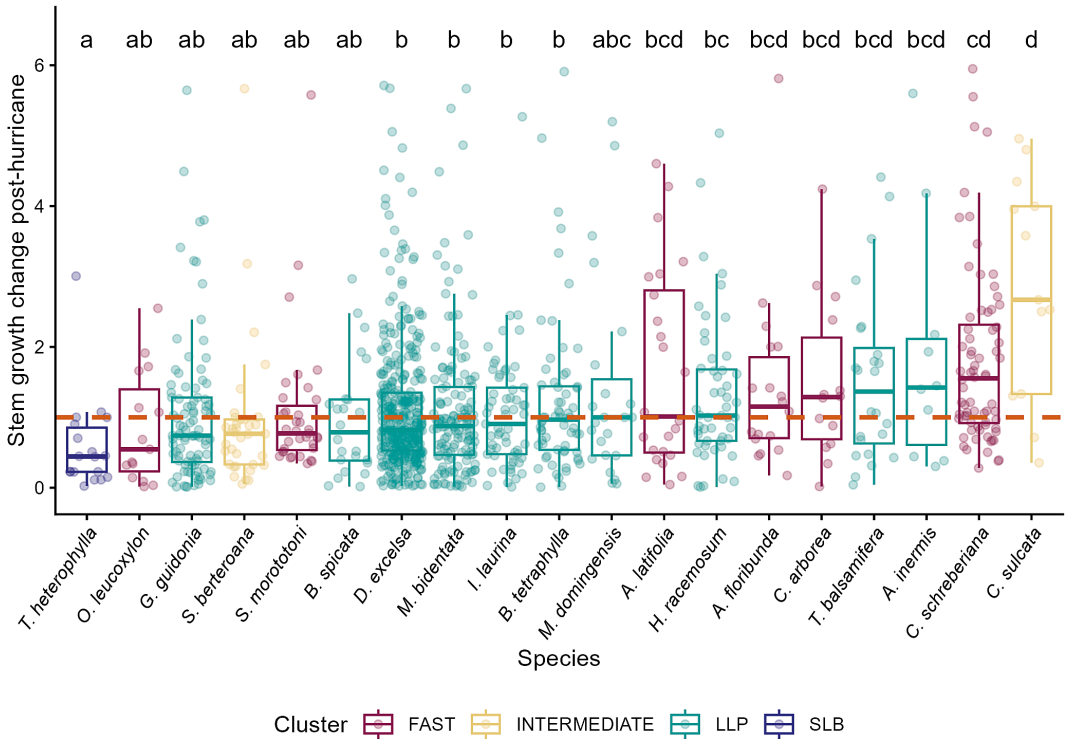

Fig. 5. Stem growth change posthurricane by species, as the ratio between posthurricane growth and prehurricane growth. The orange dashed line indicates ratio = 1, with values >1 indicating increased growth and <1 decreased growth in the posthurricane period. Individuals are colored by their species' demographic strategy, LLP = long lived pioneer; SLB = short lived breeder. Significant differences between species were tested with a Kruskal–Wallis test with BH correction for multiple comparisons; the results are indicated with letters in the box plot. Nonoverlapping letters indicate a corrected *P* value >0.05. Refer to *SI Appendix*, Table S1 for species abbreviations.

that include a damage module include a dominant negative effect of biomass loss on growth based on findings from Barro Colorado Island, a nonhurricane forest in Panama (1). However, we found only a very small negative effect of crown height loss on growth, similar to other studies from other wet hurricane forests (3, 27). Across the community, growth rates of survivors remained largely stable or even increased relative to prehurricane levels. One possible explanation is that dominant species in these hurricane-prone forests are evolutionarily adapted to recurrent disturbances and possess traits that buffer against stress and facilitate recovery (47). This highlights the need to study the effects of crown damage on demography across different biogeographical contexts, including dryer forests (29, 48), since assumptions based on one ecosystem are unlikely to be generalizable across forest types or regions.

Furthermore, our study demonstrates the value of integrating field-based growth measurements with airborne LiDAR (35, 49). Unlike previous remote sensing efforts focused on canopy- or plot-level impacts, our approach links tree-level crown damage to stem growth trajectories (34, 49). This integration connects structural disturbance to demographic performance, helping to assess shifts in growth trends after disturbance (35). By combining growth censuses with remote sensing data, we also overcome the limitations of posthurricane field-based damage assessments and we can directly quantify individual tree recovery over time. Together, these approaches deepen our mechanistic understanding of how crown damage influences tree growth and forest resilience. Notably, our results show that severe structural damage does not necessarily lead to immediate mortality as some trees lost up to 86% of their crowns yet remained alive 5 y later. Furthermore, crown height loss in the neighborhood was only weakly correlated with basal area loss as estimated from mortality in the field census (Pearson's r = 0.28; *SI Appendix*, Fig. S2). This highlights the ongoing challenge of defining reliable remote sensing thresholds for tree death.

From a carbon dynamics perspective, our findings suggest that the primary effects of hurricanes in this forest are expressed through abiotic effects on soil processes (50, 51), biomass loss and decomposition (9, 19, 52, 53), and mortality (2, 25), rather than through persistent negative effects on the growth of surviving individuals. Structural damage, quantified here as crown height loss, did reduce posthurricane growth, but the magnitude of this effect was small. Nonetheless, substantial crown loss is likely to alter individual carbon balance (1), potentially over timescales longer than those captured in our study. Understanding how crown damage drives both immediate and delayed mortality is therefore critical (15), as these dynamics coupled with growth of damaged survivors are the dominant drivers of hurricane impacts on biomass at the stand level. As disturbance frequency increases under future climates, cumulative stress could progressively reduce tree resources, eventually amplifying growth declines (54) and mortality. Yet the dominant canopy species (*D. excelsa*, *M. bidentata*, and *Guarea guidonia*) maintained stable growth rates and saw mortality rates of only 20% and 18% (*SI Appendix*, Table S1), even with this category 4 storm. This highlights the resilience of these dominant taxa and suggests that the forest's core contributors to carbon storage can maintain growth rates under severe disturbances.

Materials and Methods

Study Site. This study was conducted in the long-term, 16-ha LFDP (SW corner 18° 20′ N, 65° 49′ W), located in the Luquillo mountains of northeastern Puerto Rico (55). The site is classified as subtropical wet forest (56) and is characteristic of the tabonuco forest zone, named for its dominant canopy species (*D. excelsa*). Mean annual rainfall is approximately 3,500 mm, mean temperature is 25.2 °C,

and elevation ranges from 333 to 428 m a.s.l. The LFDP has experienced multiple natural and anthropogenic disturbances over the past century. Before 1934, portions of the plot were lightly logged and farmed for household agriculture (55), but forest structure and canopy cover have since recovered. In the past 50 y, the LFDP has also experienced three major hurricanes: Hugo in 1989, Georges in 1998, and María in September 2017. Basal area was estimated to average 36.7 m^2 ha^{-1} at the time of hurricane Hugo, 30.85 m^2 ha^{-1} at the time Georges struck, and 38.37 m^2 ha^{-1} in 2016, the year before María struck the forest.

Growth and Location Data. All stems ≥ 20 cm DBH in the LFDP have been mapped and measured at 5-y intervals since 1990, available from the Luquillo LTER (57). For this analysis, we quantified stem growth between census 5 (2011) and census 6 (2016; "prehurricane") and between census 6 and census 7 ("posthurricane"). Stem densities particularly of small stems increased substantially following H. María, leading to an extended duration of census 7, which began in the second half of 2021 and was completed mid-2023 (Fig. 1*B*). Therefore, posthurricane growth was calculated as the total growth between censuses 6 and 7 divided by the time interval between measurements for each tree, then converted to an annual rate by multiplying by 365. The same procedure was used to calculate prehurricane growth between censuses 5 and 6. Our prehurricane estimate spans the 2015–2016 drought period, which temporarily reduced growth rates across the site (40, 58). However, drought impacts were modest and species-specific, and most trees exhibited partial recovery in 2016 (40, 59). We therefore consider prehurricane growth a valid reference for comparison with posthurricane growth. Because of the extended duration of census 7, we tested whether "census duration" (the number of days between each tree's census 6 and 7 measurements) affected absolute growth, as trees measured later in 2023 had more time to recover from hurricane damage than those measured in 2021. We indeed found a small but significant positive correlation between census duration and absolute posthurricane growth (Pearson r = 0.15, df = 1080, P <0.01). Consequently, census duration was included as a covariate in all subsequent models analyzing growth responses.

Crown Height from LiDAR. The most evident structural impact of a hurricane is the reduction in tree height (60). Therefore, to quantify crown damage, we used airborne LiDAR data collected by the G-LiHT Airborne Imager (61) to calculate crown height loss. Data acquisition occurred in March 2017 (prehurricane), April 2018 (7 mo posthurricane), and March 2020 (2.5 y posthurricane Fig. 1*B*). All three surveys employed the same G-LiHT v2 system, equipped with two VQ-480i scanning LiDAR units (Riegl Laser Measurement Systems, Horn, Austria) and an additional high-resolution camera to provide 3-cm resolution RGB imagery (Phase One, Copenhagen, Denmark) (61). Flights were conducted at a nominal altitude of 335 m above ground level and a speed of 130 kn, producing laser footprints approximately 10 cm in diameter (1,550 nm wavelength) and with an average sampling density of 12 pulses per square meter. Pre- and postflight boresight alignment ensured vertical measurement accuracy within 10 cm (1 sigma) across all campaigns. CHM were calculated as the difference between the digital terrain model (elevation of the ground) and the digital surface model (elevation of the canopy surface) (34). The RGB imagery as well as the processed terrain and CHM (1 m resolution) from the G-LiHT missions are publicly accessible through the G-LiHT data portal (https://gliht.gsfc.nasa.gov) (61). Slope and TWI were calculated from the LiDAR-derived Digital Elevation Model for all trees in the LFDP based on their locations.

To identify individual tree crowns, we combined the tree height model derived from the 2017 G-LiHT flights with the high-resolution aerial RGB images from same flights. First, all crowns within the LFDP in 2017 were manually delineated from the RGB images (62). This resulted in 3,855 delineated crowns (63), which closely aligns with the number of stems over 20 cm DBH recorded in the 2016 field census of the LFDP (which are the trees we expect to reach the canopy). The quality of the manual delineations was validated with three different independent sources: a crowd-sourced crown segmentation on Amazon Mechanic Turk (MTurk); a smaller-scale accurate manual crown segmentation with additional help of high-precision field measurements for 124 trees, and the census data from the LFDP (for details see refs. 45, 63).

Field mapped stem locations in the LFDP are derived using the high-precision georeferenced locations of the four corners of the 16-ha plot, and a grid imposed on the 16 ha using field surveying techniques. The survey divided the 16-ha plot into 400 20 × 20 m plots. Each 20 × 20 plot was further subdivided into 16 5 × 5 subquadrats, and each tree was mapped within each subquadrat. Using a stepwise process, we then manually matched the delineated crown polygons to mapped tree stems in the LFDP from the 2016 census. The method is visualized in *SI Appendix*, Fig. S3, showing the tree stems and delineated crowns. Manual crown-to-tree assignment was necessary because only a fraction of the stems censused in the LFDP are visible in the canopy, and most canopy polygons contained several candidate stem points within them, as seen in *SI Appendix*, Fig. S3. Furthermore, normal surveying errors, tree growth patterns, and the complex topography of the site led to imprecise field mapped stem locations.

For the manual crown-to-tree mapping, the LiDAR-derived crown polygons and the field stem position points were superimposed on the RGB images of the LFDP from 2017. The 3,855 crown polygons had initial species designations that had been algorithmically assigned. Using a spatially sequential approach, polygon species assignments were corrected based on visually distinctive species characteristics. Crown polygons were then matched to individuals based on species visual canopy characteristics, size, and physical proximity to previous tree assignments. The first stem assignments matched large canopy polygons to the largest DBH individuals, on the assumption that these were most likely to match canopy-height trees. Multiple passes over an area were used to assign progressively smaller trees, using relative distance to already-assigned trees as additional information when there were multiple candidate stems for a polygon. Remaining crowns where multiple stem candidates in the vicinity of the crown polygon made identification uncertain were excluded from the analysis. This resulted in 3,501 crowns matched to individual trees in the LFDP.

Next, we refined the identified crown polygons using the ForestTools package (64) in R by integrating the canopy height model, guided by the crown centroids from the manual delineations. This step allowed better separation of neighboring crowns that were difficult to distinguish visually from the RGB imagery alone. Finally, the resulting ForestTools delineations were manually updated once more to exclude adjacent tree crowns that were unusually flat and had been erroneously merged by ForestTools, such as instances involving individuals of *C. schreberiana*. Using the centroids of these polygons for 2017 as a starting point, we then again used the ForestTools package with the CHM to create crown delineations for the same trees in 2018 and 2020. In all ForestTools delineation steps, the minimum height was set to five meters, assuming any vegetation below five meters was not part of the crown. This automatically excluded major tree fall gaps in the posthurricane delineations for 2018. Crown segmentation based on the full LiDAR point cloud and an automatic 3D crown delineation algorithm (AMS3D) found very similar canopy damage estimates to this estimation based on manual delineations and the CHM (63).

Crown Damage Variables. Using the crown polygons corresponding to identified stems, we calculated the damage variables of interest (Fig. 1). Prehurricane crown area (m^2) and average crown height (m) were measured from the final crown polygons and the CHM of 2017. The CHM had a resolution of 1 m, so when a tree crown only partially overlapped with a pixel, we calculated the proportion of that pixel covered by the crown. The average crown height was then derived by averaging canopy heights across all intersecting pixels, weighted by the proportion of each pixel covered by the crown. Percentage crown height loss between 2017 and 2018 was calculated from the 2017 crown polygons, using the average crown height in that polygon in 2017 and in 2018, as [(height '17–height '18)/height '17] × 100%. Additionally, we calculated posthurricane crown heights in 2018 and 2020 from the crown polygons from 2018 and 2020. These data were used to calculate crown height recovered posthurricane (m), as (height '20–height '18). Additionally, we calculated average canopy height in the neighborhood, using a 5 m buffer around each polygon in 2017 and 2018. We also tested our models using the same variables but with a buffer width of 10, 15, and 20 m, to test the robustness of this distance cutoff. The results of the Bayesian models (see *Statistical Analysis* below) were the same for all buffer distances, so we chose 5 m as the size that best captures the potential positive effect of decreased competition, as well as the potential negative effect of increased temperatures and potential drought stress. The neighborhood heights were used to compute percentage average neighborhood height loss between 2017 and 2018. The difference between focal tree in 2018 and neighborhood height was used to calculate the relative height difference of the focal tree in 2018. Last, we also calculated the live basal area that was lost in the 5 m neighborhood due to mortality from field data by comparing alive and dead trees in census 6 (2016)

and a damage census that was done posthurricane (2018). We identified all stems in the 5 m buffer around each focal tree from their field mapped locations and calculated the basal area (%) that was lost between 2016 and 2018 because the trees died.

Given the challenges of accurately matching crowns with their corresponding trees and to ensure data quality, we excluded stems from the 3,501 matched crowns based on several criteria. Trees that died between the field damage assessment and the seventh census were removed due to the absence of post-hurricane growth data (n = 974). We also removed stems with a DBH (1.30 m) <20 cm in the census in 2016, as identifying crowns of smaller trees is particularly difficult, even if they reach the canopy (n = 93). All palms (n = 361) and *Ficus* (n = 14) species were excluded because their stem diameter increases do not reliably indicate growth. We also excluded trees where the field damage assessment from 2018 (see ref. 25) differed substantially from the percentage height loss estimated remotely, as this discrepancy strongly suggests incorrect crown-to-tree matching. Specifically, stems with measured crown loss >90% but classified as "Light damage" in the field (n = 3) and those with crown loss <10% but recorded as "Heavy damage" (n = 149), were removed. While these cutoffs are intentionally wide, reflecting the different sources and inherent uncertainties of the two datasets, they provide a conservative way for ensuring that trees with clearly inconsistent crown-to-tree identifications are excluded from the analysis. Furthermore, we excluded crowns with an area smaller than 4 m^2 in 2017, 2018, or 2020 because accuracy is likely too small for those crowns (n = 219) (34), as well as trees with missing growth rates (n = 485), mostly because the main stem broke but resprouted, resulting in a living tree with a DBH 20 cm in 2016, but not in the subsequent census between 2021 and 2023. We also removed trees exhibiting anomalous posthurricane growth rates (<−1 cm/y or >4 cm/y, n = 45) since these outliers were verified as measurement errors. Last, we removed individuals from species that had <10 remaining individuals (n = 76). This led to a final dataset of 1,082 individuals of 19 species (*SI Appendix*, Table S1).

Statistical Analysis. To assess the impact of hurricane damage on stem growth, we used two complementary measures: absolute growth and stem growth change. Absolute growth represents stem growth recorded within the census period that included the hurricane (2017), capturing primarily posthurricane growth (2016–2021–2023). In contrast, stem growth change measures the relative shift in growth before and after the hurricane, calculated as a post/pre-ratio using prehurricane growth (2011 to 2016) and posthurricane growth (2016–2021–2023). Values >1 indicate increased growth in the posthurricane period. Both measures provide distinct but valuable insights into the effects of hurricane damage. Absolute growth highlights the overall "winners" after the hurricane by identifying which trees grew the most across the community. Stem growth change, on the other hand, captures individual-level responses: how a given tree's growth shifted posthurricane and which factors influence the extent of that shift.

We first tested for an effect of period (pre- versus posthurricane) on absolute growth (Q1). The response variable in this model was annual growth rate, with two values for each tree from the two census periods (pre- and posthurricane growth). We developed a Bayesian model using a hurdle gamma distribution, as the growth values are strictly nonnegative and the data contained a large number of zeros. The hurdle part of the model captures whether growth was zero vs. nonzero, while the gamma part models the magnitude of nonzero growth. We included census duration as a covariate to account for the differences in time between censuses. For both the hurdle and the gamma part, we modeled growth as a function of Species * Period, using Tree ID as a random factor to account for repeated measurements. A significant interaction between the two variables indicates that growth post hurricane was significantly different from prehurricane growth in that species.

To evaluate the effects of the different damage and location variables, we used a Structural Causal Modeling Framework (65–69). We constructed a causal diagram (DAG; *SI Appendix*, Fig. S1) to assess the direct causal effect of each predictor variable on the outcome of interest. This DAG represents our hypotheses regarding how the damage variables influencing both absolute and stem growth change are related. After developing the DAG, we tested the testable implications and confirmed the DAG was consistent with the data. We applied the so-called "backdoor criterion" to the DAG using the *daggity* package (70), resulting in a minimal set of control variables for each variable for which we wanted to estimate its association with growth (65). This approach allowed us to condition the statistical models on control variables based on the DAG, which closed any noncausal paths between exposure and outcome variable (see ref. 66 for more information on DAG analyses).

Then, to test for a nonlinear effect of damage (Q2), we developed a Bayesian model using the post/pre-growth ratio as the response variable. The predictors were all standardized and included individual height loss, its quadratic term (to assess nonlinear effects), height recovered, neighborhood height loss, and the relative canopy height of the focal tree compared to its neighbors, as defined by the study's DAG (*SI Appendix*, Fig. S1). The model used an ex-Gaussian distribution with an identity link function to accommodate the skewness in the data. Species identity was included as a random intercept to account for species-level variation. This hierarchical structure explicitly accounts for unequal sample sizes by estimating species-level variance while allowing each observation to contribute according to its within-species variability. We chose not to apply additional abundance-based weighting, as it would shift the interpretation from individual-level growth responses to community-weighted means, which was not the primary objective of this analysis.

Pairwise correlations showed that none of the predictor variables were highly correlated ($R^2 < 0.52$) allowing them to be safely included in the model (71). The only variables that showed a slightly higher correlation were individual height loss and neighborhood height loss, with a correlation of 0.57. To test whether this led to collinearity problems, variance inflation factors (VIF) were calculated via a frequentist model using the glmmTMB package (72) using the same set of predictors, since brms does not compute VIF. All predictor variables had VIF values below 3, confirming low collinearity.

We continued with additional Bayesian models to test for the effects of all predictors (individual and neighborhood damage effects, Fig. 1) on the two outcome variables (Q3; *SI Appendix*, Table S2), absolute stem growth and stem growth change posthurricane. We modeled absolute posthurricane growth using a hurdle gamma distribution (as in Q1). For both components (hurdle component and gamma component), we included the same set of predictors in each model (*SI Appendix*, Table S2). Stem growth change was modeled using an ex-Gaussian distribution (as in Q2). The differing treatment of species across analyses reflects distinct model purposes: for the community-wide analysis (Q1), modeling species and period as interacting fixed effects allowed for direct hypothesis testing of species-specific temporal shifts. In contrast, for the damage models (Q2 and Q3), species identity was treated as a random intercept to control for structured biological variation while focusing inference on damage variables.

In initial model development, we evaluated whether adding species-specific slopes improved model performance. However, leave-one-out cross-validation comparisons showed no improvement from the inclusion of random slopes. Therefore, the final models retained only species-specific intercepts. For all models, species was included as a random factor and census duration was included as a covariable for all models on absolute growth (*Growth and Location Data*). Model fit and adequacy were evaluated per model through posterior predictive checks based on 500 draws from the posterior predictive distribution (*SI Appendix*, Figs. S6 and S7), which confirmed that all models provided good fits to the observed data.

All Bayesian models were developed using the brms package in R (73). Each model fitting was performed with three Markov Chain Monte Carlo chains, with 800 iterations and 200 warm-up steps, using the cmdstanr backend. We used noninformative priors and all numerical predictor variables were standardized (z-scores) prior to analysis.

To test for species-specific differences in stem growth changes (Q4), we used the nonparametric Kruskal–Wallis test. Following a significant test result, we conducted pairwise post hoc comparisons using Dunn's test with Benjamini–Hochberg *P*-value adjustment to control for false discovery rate. For visualization, species were grouped by their demographic strategies based on data from the LFDP (74, 75), including: species with fast strategy (pioneers), intermediate species, long lived pioneers, and short lived breeders (*SI Appendix*, Table S1).

Because these demographic strategies are based on specific species traits and variation exists within each group, we also tested whether specific species traits were associated with stem growth change (76). We evaluated associations with Specific Leaf Area, leaf N content (%), leaf P content (%), wood density

(g/cm^3), seed size (g), and Leaf Area Index based on species mean values (77), using species average stem growth change per species as response variable (n = 19) in Bayesian models as those for Q3. However, we found no effect of any of these traits on stem growth change. Given that these traits, especially specific leaf area and leaf nutrient content, can vary considerably within species (78), we decided not to include these analyses in the main results, and future work should measure these traits at the level of individual surviving trees. As such, this trait-based analysis could be regarded as preliminary.

Field Damage Comparison. Last, we compared the damage assessment from the LiDAR data to the field damage assessment. In the field assessment, which took place within 8 mo after H. María had passed, damage was classified per tree as Light (<25% crown lost), Medium (25 to 75%), or Heavy (>75%). We found that those categories aligned well with the damage assessment from the LiDAR data: median crown height lost from LiDAR increased from the Light to the Medium and Heavy categories (*SI Appendix*, Fig. S4). As each method has its limitations (field assessments lack information about prehurricane conditions, and LiDAR may not always accurately distinguish between individual tree crowns), this overall alignment of the damage assessments between the methods lends support to the validity of our analysis.

Additionally, we tested for an effect of damage category from the field assessment on stem growth change, separate from the LiDAR-based damage assessment. For this analysis we included all trees >20 cm DBH in the 2016 field census that were still alive in the following census. We selected all trees from the same species we had included for the LiDAR based assessment (*SI Appendix*, Table S1) and removed trees with abnormal growth measurements (<−1 cm annually), resulting in a dataset of 3,812 trees. We then developed a Bayesian model, defined as: Stem growth change ~Damage class + (1 | Species). We used an ex-Gaussian distribution, like the previous models for relative stem growth change. We also tested a version of this model with the exact same dataset as had been used previously (1,082 trees) and confirmed that our findings on the effect of damage category on stem growth change were the same with both datasets (*SI Appendix*, Fig. S5): we found a significant negative effect of increasing damage on stem growth change (CI for Medium damage −0.14 to −0.05, mean estimate −0.10; CI for Heavy damage −0.30 to −0.19; mean estimate −0.25). All statistical analyses were conducted in R Software (79).

Data, Materials, and Software Availability. Original LiDAR data used for this study are available online at https://gliht.gsfc.nasa.gov (61). Tree census data can be found at https://portal.edirepository.org/nis/mapbrowse?scope=knb-lter-luq&identifier=119&revision=1545980 (57). The processed data and R code used in this study to replicate the main analyses and results are available at 10.5281/zenodo.18657455 (80). All other data are included in the manuscript and/or *SI Appendix*.

ACKNOWLEDGMENTS. Collection of tree damage data was supported by National Science Foundation RAPID award DEB-1801315 to J.K.Z. and M.U. The census of the Luquillo Forest Dynamics Plotfollowing Hurricane María was supported by National Science Foundation award DEB-2028688 to J.K.Z. and M.U. Additional support was provided by National Science Foundation awards DEB-9705814 to the Luquillo Long-Term Ecological Research (LTER). G.A. collected post-María Hurricane data as part of the Next Generation Ecosystem Experiments-Tropics, funded by the United States Department of Energy, Office of Science, Office of Biological and Environmental Research. Funding for acquisition and processing of the LiDAR data was provided by the Department of Energy (Terrestrial Ecosystem Science Program, Interagency Agreements with the United States Forest Service 89243018SSC000012 and with National Aeronautics and Space Administration 89243018SSC000013, and from the Next Generation Ecosystem Experiment-Tropics, Office of Biological and Environmental Research) and by the U.S. Department of Agriculture (USDA) Forest Service, United States Department of Interior, National Institute of Food and Agriculture 2018–67,030–28,124, and National Aeronautics and Space Administration. The USDA Forest Service International Institute of Tropical Forestry, Luquillo LTER, and National Aeronautics and Space Administration's Airborne Science Program provided logistical support.

Author affiliations: [a]Department of Ecology, Evolution and Environmental Biology, Columbia University, New York, NY 10027; [b]Q-ForestLab, Department of Environment, Faculty of Bioscience Engineering, Ghent University, Ghent 9000, Belgium; [c]Department of Ecology and Evolutionary Biology, University of Michigan, Ann Arbor, MI 48109; [d]Oikobit Limited Liability Company (LLC), Albuquerque, NM 87120; [e]Department of Statistics, Columbia University, New York, NY 10032; [f]Department of Geographical Sciences, University of Maryland, College Park, MD 20742; [g]Biospheric Sciences Laboratory, NASA Goddard Space Flight Center, Greenbelt, MD 20771; [h]Department of Biostatistics, City University of Hong Kong, Kowloon, Hong Kong; and [i]Department of Environmental Sciences, Universidad de Puerto Rico, San Juan, PR 00925

1. J. F. Needham *et al.*, Tree crown damage and its effects on forest carbon cycling in a tropical forest. En. *Global Change Biol.* **28**, 5560–5574 (2022).
2. G. Arellano *et al.*, Crown damage and the mortality of tropical trees. *New Phytol.* **221**, 169–179 (2019).
3. E. V. J. Tanner *et al.*, Long-term hurricane damage effects on tropical forest tree growth and mortality. *Ecology* **95**, 2974–2983 (2014).
4. M. Uriarte *et al.*, A neighborhood analysis of tree growth and survival in a hurricane-driven tropical forest. *Ecol. Monogr.* **74**, 591–614 (2004).
5. S. L. Yap *et al.*, Dynamic response of a Philippine dipterocarp forest to typhoon disturbance. *J. Veg. Sci.* **27**, 133–143 (2016).
6. E. L. Chapman *et al.*, Hurricane Katrina impacts on forest trees of Louisiana's Pearl River basin. *For. Ecol. Manage.* **256**, 883–889 (2008).
7. A. E. Lugo, Visible and invisible effects of hurricanes on forest ecosystems: An international review. *Aust. Ecol.* **33**, 368–398 (2008).
8. M. Uriarte *et al.*, 20th-Century hurricanes leave long-lasting legacies on tropical forest height and the abundance of a dominant wind-resistant palm. *Ecol. Evol.* **13**, e10776 (2023).
9. A. W. Quebbeman *et al.*, A severe hurricane increases carbon dioxide and methane fluxes and triples nitrous oxide emissions in a tropical forest. *Ecosystems* **25**, 1754–1766 (2022).
10. J. Hall *et al.*, Forest cover lessens the impact of drought on streamflow in Puerto Rico. *Hydrol. Process* **36**, e14551 (2022).
11. K. Bhatia *et al.*, A potential explanation for the global increase in tropical cyclone rapid intensification. *Nat. Commun.* **13**, 6626 (2022).
12. T. Knutson *et al.*, Tropical cyclones and climate change assessment: Part II: Projected response to anthropogenic warming. *Bull. Am. Meteorol. Soc.* **101**, E303–E322 (2020).
13. N. G. McDowell *et al.*, Pervasive shifts in forest dynamics in a changing world. *Science* **368**, eaaz9463 (2020).
14. I. T. M. Network, Towards a global understanding of tree mortality. *New Phytol.* **245**, 2377–2392 (2025).
15. D. Zuleta *et al.*, Individual tree damage dominates mortality risk factors across six tropical forests. *New Phytol.* **233**, 705–721 (2022).
16. Y. Pan *et al.*, The enduring world forest carbon sink. *Nature* **631**, 563–569 (2024).
17. A. H. Eckes-Shephard *et al.*, Demography, dynamics and data: Building confidence for simulating changes in the world's forests. *New Phytol.* **248**, 2722–2749 (2025).
18. J. Clark *et al.*, "Disturbance and vegetation dynamics in Earth System Models: Workshop report" (Tech. Rep. DOE/SC–0196, USDOE Office of Science, United States, 2018).
19. M. Shi *et al.*, Assessing simulations of forest hurricane disturbance and recovery in Puerto Rico by ELM-FATES using field measurements. en. *J. Geophys. Res. Biogeosci.* **130**, e2024JG008350 (2025).
20. J. Zhang *et al.*, The impact of hurricane disturbances on a tropical forest: Implementing a palm plant functional type and hurricane disturbance module in ED2-HuDi V1.0. *Geosci. Model Dev.* **15**, 5107–5126 (2022).
21. R. Seidl *et al.*, Modelling natural disturbances in forest ecosystems: A review. *Ecol. Model.* **222**, 903–924 (2011).
22. L. Wu *et al.*, Sensitivity analysis of the typhoon disturbance effect on forest dynamics and carbon balance in the future in a cool-temperate forest in northern Japan by using SEIB-DGVM. *For. Ecol. Manage.* **451**, 117529 (2019).
23. S. E. Russo *et al.*, The interspecific growth–mortality trade-off is not a general framework for tropical forest community structure. *Nat. Ecol. Evol.* **5**, 174–183 (2021).
24. S. Kambach *et al.*, Consistency of demographic trade-offs across 13 (sub)tropical forests. *J. Ecol.* **110**, 1485–1496 (2022).
25. M. Uriarte *et al.*, Hurricane María tripled stem breaks and doubled tree mortality relative to other major storms. *Nat. Commun.* **10**, 1362 (2019).
26. J. B. Cannon *et al.*, Hurricane wind regimes for forests of North America. *Proc. Natl. Acad. Sci. U.S.A.* **120**, e2309076120 (2023).
27. J. Altman *et al.*, Forest response to increasing typhoon activity on the Korean peninsula: Evidence from oak tree-rings. *Global Change Biol.* **19**, 498–504 (2013).
28. J. C. Rodgers III *et al.*, Tropical cyclone signals within tree-ring chronologies from Weeks Bay National Estuary and Research Reserve, Alabama. *J. Coast. Res.* **2006**, 1320–1329 (2006).
29. D. Imbert, J. Portecop, Hurricane disturbance and forest resilience: Assessing structural vs. functional changes in a Caribbean dry forest. *For. Ecol. Manage.* **255**, 3494–3501 (2008).
30. C. S. Tucker *et al.*, Tropical cyclone response in annual tree growth at three different coastal sites along the Gulf of Mexico, USA. *Forests* **16**, 476 (2025).
31. V. Trouet *et al.*, Shipwreck rates reveal Caribbean tropical cyclone response to past radiative forcing. *Proc. Natl. Acad. Sci. U.S.A.* **113**, 3169–3174 (2016).
32. C. D. Canham *et al.*, Variation in susceptibility to hurricane damage as a function of storm intensity in Puerto Rican tree species. *Biotropica* **42**, 87–94 (2010).
33. J. K. Zimmerman *et al.*, Responses of tree species to hurricane winds in subtropical wet forest in Puerto Rico: Implications for tropical tree life histories. *J. Ecol.* **82**, 911 (1994).
34. V. Leitold *et al.*, Tracking the rates and mechanisms of canopy damage and recovery following Hurricane Maria using multitemporal lidar data. *Ecosystems* **25**, 892–910 (2022).
35. K. Calders *et al.*, Realistic virtual forests for understanding forest disturbances and recovery from space. *ISPRS J. Photogramm. Remote Sens.* **227**, 501–507 (2025).

36. E. R. Boose *et al.*, Landscape and regional impacts of hurricanes in Puerto Rico. *Ecol. Monogr.* **74**, 335–352 (2004).
37. N. B. Schwartz *et al.*, Topography and traits modulate tree performance and drought response in a tropical forest. *Front. For. Glob. Change* **3**, 596256 (2020).
38. T. R. Knutson *et al.*, Tropical cyclones and climate change. *Nat. Geosci.* **3**, 157–163 (2010).
39. K. Ogle *et al.*, Quantifying ecological memory in plant and ecosystem processes. *Ecol. Lett.* **18**, 221–235 (2015).
40. M. N. Umaña, G. Arellano, Legacy effects of drought on tree growth responses to hurricanes. *Ecography* **44**, 1686–1697 (2021).
41. D. M. P. Peltier, K. Ogle, Tree growth sensitivity to climate is temporally variable. *Ecol. Lett.* **23**, 1561–1572 (2020).
42. H. Hartmann, S. Trumbore, Understanding the roles of nonstructural carbohydrates in forest trees–From what we can measure to what we want to know. *New Phytol.* **211**, 386–403 (2016).
43. D. T. Cayetano *et al.*, Cyclones reduce growth and mortality differences between liana-laden and liana-free trees in Belize. *J. Ecol.* **113**, 2386–2400 (2025).
44. D.-L. Cheng *et al.*, Scaling relationship between tree respiration rates and biomass. *Biol. Lett.* **6**, 715–717 (2010).
45. R. Ankori-Karlinsky *et al.*, Wind acclimation in a subtropical forest: Trees on wind-exposed slopes are shorter with smaller crowns. *New Phytol.* **247**, 1643–1654 (2025).
46. W. L. Silver *et al.*, Soil oxygen availability and biogeochemistry along rainfall and topographic gradients in upland wet tropical forest soils. *Biogeochemistry* **44**, 301–328 (1999).
47. M. P. Griffith *et al.*, Cyclone tolerance in New World Arecaceae: Biogeographic variation and abiotic natural selection. *Ann. Bot.* **102**, 591–598 (2008).
48. L. Poorter *et al.*, Functional recovery of secondary tropical forests. *Proc. Natl. Acad. Sci. U.S.A.* **118**, e2003405118 (2021).
49. J. Q. Chambers *et al.*, Hurricane Katrina's carbon footprint on U.S. Gulf Coast Forests. *Science* **318**, 1107–1107 (2007).
50. A. B. Shiels *et al.*, Cascading effects of canopy opening and debris deposition from a large-scale hurricane experiment in a tropical rain forest. *BioScience* **65**, 871–881 (2015).
51. A. B. Shiels *et al.*, Responses to canopy loss and debris deposition in a tropical forest ecosystem: Synthesis from an experimental manipulation simulating effects of hurricane disturbance. *For. Ecol. Manage.* **332**, 124–133 (2014).
52. J. A. Holm *et al.*, Shifts in biomass and productivity for a subtropical dry forest in response to simulated elevated hurricane disturbances. en. *Environ. Res. Lett.* **12**, 025007 (2017).
53. O. Gutiérrez del Arroyo *et al.*, Modeling the effects of increased hurricane frequency on the Tropical Forest Carbon Cycle. *Ecosystems* **27**, 1076–1089 (2024).
54. H. Li *et al.*, Quantitative analysis of multiple forest disturbances and their compound influences on tree growth in the western U.S. *Dendrochronologia* **79**, 126084 (2023).
55. J. Thompson *et al.*, Land use history, environment, and tree composition in a tropical forest. *Ecol. Appl.* **12**, 1344–1363 (2002).
56. J. Ewel, J. Whitmore, The ecological life zones of Puerto Rico and the US Virgin Islands (Research Paper ITF-018 18, USDA Forest Service, Institute of Tropical Forestry, Rio Piedras, Puerto Rico, 1973).
57. J. Zimmerman, Census of species, diameter and location at the Luquillo Forest Dynamics Plot (LFDP), Puerto Rico. EDI Data Portal. https://portal.edirepository.org/nis/mapbrowse?packageid=knb-lter-luq.119.1545980. Deposited 26 March 2026.
58. C. M. Smith-Martin *et al.*, Hydraulic traits are not robust predictors of tree species stem growth during a severe drought in a wet tropical forest. *Funct. Ecol.* **37**, 447–460 (2023).
59. P. A. Zuidema *et al.*, Pantropical tree rings show small effects of drought on stem growth. *Science* **389**, 532–538 (2025).
60. N. V. L. Brokaw, J. S. Grear, Forest structure before and after Hurricane Hugo at three elevations in the Luquillo Mountains, Puerto Rico. *Biotropica* **23**, 386 (1991).
61. B. D. Cook *et al.*, NASA Goddard's LiDAR, hyperspectral and thermal (G-LiHT) airborne imager. *Remote Sens.* **5**, 4045–4066 (2013).
62. QGIS, QGIS Geographic Information System, version 3.32.3 (Open Source Geospatial Foundation Project, 2025).
63. T. Han *et al.*, Taller trees experienced less crown damage during a severe hurricane in a tropical forest. *Glob. Change Biol.* **32**, e70709 (2026).
64. A. Plowright, ForestTools: Tools for analyzing remote sensing forest data (Version 1.0.3, R package, 2025).
65. B. X. Pinho *et al.*, Winner–loser plant trait replacements in human-modified tropical forests. *Nat. Ecol. Evol.* **9**, 282–295 (2024).
66. S. Arif, M. A. MacNeil, Applying the structural causal model framework for observational causal inference in ecology. *Ecol. Monogr.* **93**, e1554 (2023).
67. L. E. Dee *et al.*, Clarifying the effect of biodiversity on productivity in natural ecosystems with longitudinal data and methods for causal inference. *Nat. Commun.* **14**, 2607 (2023).
68. J. Pearl, *Causality: Models, Reasoning and Inference* (Cambridge University Press, 2009).
69. K. Siegel, L. E. Dee, Foundations and future directions for causal inference in ecological research. *Ecol. Lett.* **28**, e70053 (2025).
70. A. Ankan *et al.*, Testing graphical causal models using the R Package, "dagitty". *Curr. Protoc.* **1**, e45 (2021).
71. C. F. Dormann *et al.*, Collinearity: A review of methods to deal with it and a simulation study evaluating their performance. *Ecography* **36**, 27–46 (2013).
72. M. E. Brooks *et al.*, glmmTMB balances speed and flexibility among packages for zero-inflated generalized linear mixed modeling. *R J.* **9**, 378 (2017).
73. P.-C. Bürkner, Brms: An R package for Bayesian multilevel models using Stan. *J. Stat. Softw.* **80**, 1–28 (2017).
74. N. Rüger *et al.*, Beyond the fast-slow continuum: Demographic dimensions structuring a tropical tree community. *Ecol. Lett.* **21**, 1075–1084 (2018).
75. M. N. Umaña *et al.*, Demographic trade-offs and functional shifts in a hurricane-impacted tropical forest. *Ann. Bot.* **131**, 1051–1060 (2023).
76. H. Paz *et al.*, Understanding hurricane resistance and resilience in tropical dry forest trees: A functional traits approach. *For. Ecol. Manage.* **426**, 115–122 (2018).
77. N. G. Swenson, M. N. Umaña, Data from: Interspecific functional convergence and divergence and intraspecific negative density dependence underlie the seed-to-seedling transition in tropical trees. (2015). https://datadryad.org/dataset/doi:10.5061/dryad.j2r53. Accessed 26 March 2026.
78. D. Zuleta *et al.*, Interspecific and intraspecific variation of tree branch, leaf and stomatal traits in relation to topography in an aseasonal Amazon forest. *Funct. Ecol.* **36**, 2955–2968 (2022).
79. R core team, R: A language and environment for statistical computing (R version 4.4.1, R Foundation for Statistical Computing Vienna, Austria, 2024).
80. L. E. Boeschoten *et al.*, Dataset Accompanying the Study by Boeschoten et al. 'Tree growth after a major hurricane reflects pre-disturbance vigor rather than canopy damage'. Zenodo. https://zenodo.org/records/18657455. Accessed 26 March 2026.